Object segmentation from *common fate*: Motion energy processing enables human-like zero-shot generalization to random dot stimuli

Matthias Tangemann **Matthias Kümmerer** **Matthias Bethge**

University of Tübingen, Tübingen AI Center
`matthias.{lastname}@bethgelab.org`

Abstract

Humans excel at detecting and segmenting moving objects according to the *Gestalt* principle of "common fate". Remarkably, previous works have shown that human perception generalizes this principle in a zero-shot fashion to unseen textures or random dots. In this work, we seek to better understand the computational basis for this capability by evaluating a broad range of optical flow models and a neuroscience inspired motion energy model for zero-shot figure-ground segmentation of random dot stimuli. Specifically, we use the extensively validated motion energy model proposed by Simoncelli and Heeger in 1998 which is fitted to neural recordings in cortex area MT. We find that a cross section of 40 deep optical flow models trained on different datasets struggle to estimate motion patterns in random dot videos, resulting in poor figure-ground segmentation performance. Conversely, the neuroscience-inspired model significantly outperforms all optical flow models on this task. For a direct comparison to human perception, we conduct a psychophysical study using a shape identification task as a proxy to measure human segmentation performance. All state-of-the-art optical flow models fall short of human performance, but only the motion energy model matches human capability. This neuroscience-inspired model successfully addresses the lack of human-like zero-shot generalization to random dot stimuli in current computer vision models, and thus establishes a compelling link between the Gestalt psychology of human object perception and cortical motion processing in the brain.
Code, models and datasets are available at `https://github.com/mtangemann/motion_energy_segmentation`.

1 Introduction

Motion is a powerful cue that humans use to detect and segment visual objects. A striking example are camouflaged animals, which are difficult to spot when stationary but become much easier to detect when moving. Motion segmentation in humans is believed to be driven by the principle of common fate [47, 48, 42], which posits that elements that move together, belong together. Remarkably, human perception generalizes this principle in a zero-shot fashion to novel textures or moving random dots. For example, the seminal work by Johansson [19] showed that humans can easily detect biological motion from only few moving dots. More recently, Robert et al. [31] introduced random dot stimuli called *object kinematograms* that preserve the motion in a video while ensuring that static appearance cues are uninformative about the video contents (Fig. 1, example video in the supplemental material).

38th Conference on Neural Information Processing Systems (NeurIPS 2024).

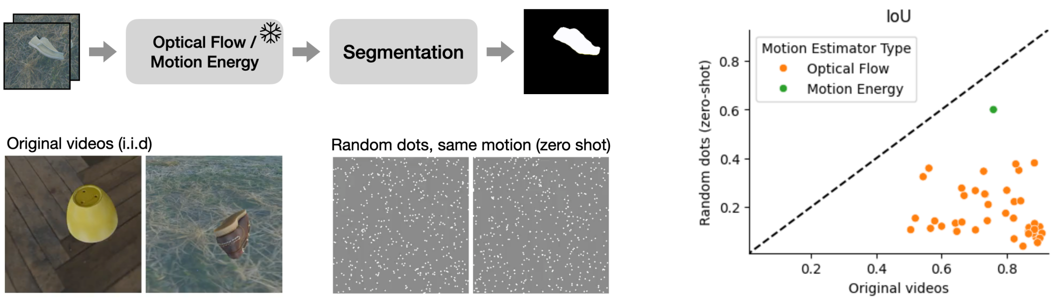

Figure 1: We compare state-of-the-art optical flow estimators and a neuroscience inspired motion energy model on a figure-ground segmentation task. For evaluation, we use random dot stimuli with the same motion patterns as the original videos, but for which the appearance of each individual frame is informative (example video in the supplemental material). The neuroscience inspired model generalizes to these stimuli much better than state-of-the-art optical flow models.

Nevertheless, humans were able to classify the animals and objects in these videos based on motion information alone.

In this work, we seek to understand the computational basis for appearance-agnostic motion perception in humans which enables this zero-shot generalization to random dots. Recent advancements in computer vision models for motion segmentation enable accurate segmentation of moving objects in natural videos based on a combination of optical flow estimation networks with downstream segmentation networks (e.g., [51]). However, it remains untested whether these models generalize in a similar way as human perception. Since the motion estimation stage is critical for segmenting moving objects, we focus on testing a broad range of state-of-the-art optical flow methods in combination with a fixed segmentation network. Our analysis reveals that existing computer vision approaches do not generalize in a human-like manner: Many high-performing models on natural stimuli perform near chance level for random dots.

In the primate visual cortex, area MT is known to be involved in motion perception and interpretation. Computational models for this area based on *motion energy* were proposed almost forty years ago [1, 46] and since then have been shown to predict key characteristics of neural firing patterns [37]. Instead of matching deep features between two frames, these models rely on spatio-temporal filtering in pixel space combined with a post-processing stage to resolve ambiguities. We demonstrate that this mechanism can be successfully integrated with deep neural networks for motion segmentation in realistic videos and reaches the performance of early deep learning based optical flow models on the original, textured videos—which is remarkable considering that the motion energy model was developed to explain the tuning of individual neurons and has several orders of magnitude fewer parameters than typical optical flow networks. Crucially, the motion energy model substantially outperforms all tested optical flow models in zero-shot generalization to moving random dots. In a direct comparison with humans in a controlled psychophysics study, the motion energy based approach is the only model that can match human capability.

In summary, our paper makes the following contributions:

- We show that a a broad range of state-of-the-art optical flow methods do not support human-like motion segmentation that generalizes to random dot patterns.
- We demonstrate that a classical neuroscience model can be successfully integrated with deep neural networks and generalizes to random dot stimuli.
- We conduct a psychophysical experiment to directly compare random dot motion segmentation in humans and machines. While state-of-the-art optical flow models fall short of human performance, the motion energy model can match it.

These results establish a compelling link between the Gestalt psychology of human object perception and cortical motion processing in the brain, showing that a motion energy approach can overcome the lack of human-like zero-shot generalization to random dot stimuli in current computer vision models. Integrating this mechanism with state-of-the-art optical flow methods is promising path towards more robust motion estimation models.

2 Related Work

Motion energy. Modelling motion perception in humans has been frequently approached using motion energy models. These models exploit the fact that a moving pattern corresponds to oriented edges when considering a video as a spatio-temporal volume [1, 46]. Several models have been proposed that build on this principle, aiming to explain the tuning properties of neurons found in visual areas V1 and MT [37, 15, 32, 28]. With few exceptions [41, 38], these models have not been used as a motion estimation models in a computer vision context. Our work is the first to study motion energy models for moving object segmentation.

Optical flow estimation. Optical flow traditionally has been formulated as an optimization problem with the goal of finding good matches between two frames [16]. During recent years, optimization based methods have been superseded by deep neural networks that frame optical flow estimation as an end-to-end regression task. FlowNet [11] pioneered this approach with a CNN that optionally includes an explicit temporal matching operation. Following works contributed better training data and proposed coarse-to-fine architectures to predict optical flow [17, 39, 40] which lead to substantial performance improvements. More recently, models that iteratively refine a high resolution optical flow map [43, 18] and Transformer-based models [36, 53, 54] have further improved state-of-the-art. Some works have compared optical flow models to human motion perception [56, 41], however not in the context of motion segmentation.

Motion Segmentation. The typical approach to motion segmentation is using optical flow as input for a downstream segmentation model. One classic line of work computes point trajectories from optical flow and then clusters the trajectories to segment moving regions [6, 29, 20]. Classical geometric approaches to motion segmentation have been combined with deep learning in later work [4, 5]. More recently, purely deep learning based approaches have been able to improve state-of-the-art [44, 9, 22, 23, 51]. To achieve high performance on classical motion segmentation datasets, the optical flow based motion segmentation is typically combined with appearance based segmentation [9, 52]. In this work, we evaluate generalization to random dot stimuli for which appearance is not informative, so we focus on purely motion-driven approaches.

3 Methods

The aim of this work is to evaluate which computational models match the capabilities of humans for zero-shot motion segmentation of random dot patterns. We follow the standard motion segmentation approach in computer vision and first use a motion model to estimate the motion in an input video, followed by a segmentation network that predicts the foreground mask. In order for models to perform well on zero-shot segmentation of random dot patterns, it is critical that the motion estimator used by the model generalizes well to these random dot stimuli. Ideally, the motion estimator would be invariant to changes in texture. Therefore, we focus on the motion estimation stage by evaluating a broad range of optical flow models in comparison to a neuroscience inspired motion energy model. As a segmentation model, we use the same segmentation architecture for all motion estimators which we train from scratch for every model.

3.1 Optical Flow Models

We use a range of optical flow models that includes all major deep learning based approaches to optical flow estimation. FlowNet 2.0 [17] was the first CNN based model that reached the performance of classical, optimization based methods. We consider three variants of the model using different combinations of subnetworks. PWC-Net [39] introduced a multi-scale approach that combined operations from classical approaches (such as cost volumes and warping), with components from deep learning. Different from previous models, RAFT [43] is not based on a coarse-to-fine approach but rather on iterative refinement of a high resolution optical flow map derived from multi-scale correspondences. GMA [18] extends the RAFT architecture by introducing a Transformer-based module to better handle occlusions, which have been shown to be difficult for previous models. More recently, GMFlow [53, 54] and FlowFormer++ [36] have been proposed as fully Transformer-based architectures for optical flow estimation.

We use the implementations and checkpoints of these models from the MMFlow library [8], except for FlowFormer++ and GMFlow for which we use the implementations and checkpoints provided by the respective authors[1][2]. For each architecture, we consider checkpoints trained on different datasets that are common in the field, including the FlyingChairs [11], FlyingThings3d [24], Sintel [7] and KITTI [25, 26]. In total, we evaluate 40 optical flow models.

We apply the models to predict multi-scale optical flow, in order to match the multi-scale features predicted by the motion energy model. All of the optical flow models internally use several scales to predict optical flow. However, this representation is followed by non-trivial processing to combine motion information across scales, so that using this internal representation directly would most likely lead to inferior performance. Therefore we use the unmodified models and scale the final optical flow prediction to the desired resolutions using bilinear interpolation.

3.2 Motion Energy Model

Motion energy models are based on the insight that a motion pattern in a video corresponds to a spatio-temporal orientation when the video is considered as an x-y-t volume [1, 46]. The motion at every pixel can therefore be estimated by using spatiotemporal filters that respond to a particular motion direction and speed. This mechanism has important differences from the optical flow models discussed before. All of the optical flow models compute deep features for two frames individually and match these features between two frames to estimate motion. The spatio-temporal filters in motion energy models on the other hand operate directly in pixel space. This approach leads to more ambiguous matches, which are typically resolved by considering more than two frames, and a postprocessing stage.

In this study, we build on the influential motion energy model by Simoncelli & Heeger [37]. In addition to the oriented filters described above, this model introduced a second stage that implements an *intersection of constraints* construction [13, 2] in order to resolve ambiguities of the linear filter responses. This motion energy model can be implemented as a CNN with the architecture shown in Figure 2. We derived the weights of the CNN from the the parameters of the original model and verified that our PyTorch [30] implementation of the motion energy model equals the original MATLAB implementation[3] up to numerical differences. Following the original model, we apply the model for five different input scales that are obtained by repeatedly blurring and downsampling the input by a factor of two. To streamline the implementation, we do not scale the activations after every layer and experimentally verified that this change does not affect downstream performance for motion segmentation.

3.3 Segmention model

We use a coarse-to-fine segmentation network to predict per-pixel logits for the respective pixel belonging to the foreground object (Figure 2). Input to the segmentation model are the multi-scale motion energy maps or multi-scale optical flow maps as predicted by the models described earlier. At each scale, the segmentation model consists of three components: The *input projection* layer predicts motion features for each scale. The core of the network is a *refinement CNN* that aggregates features across scales. At each scale, the refinement CNN concatenates the motion features from the current scale with the refined representation from all previous scales and predicts the refined representation for the current scale. Finally, the *output projection* layer predicts the segmentation given the refined representation from the finest scale. All layers except for the output projection are followed by a CELU nonlinearity [3] and instance normalization [45]. The parameters of the components are shared across the stages, so that the network is essentially a recurrent neural network that integrates information from coarsest to the finest scale in order to predict a segmentation.

3.4 Training

All models are trained on a synthetic video dataset that we generated using the Kubric library[14]. Each video shows a single moving object in front of a moving background. The 3D objects and

[1] `https://github.com/XiaoyuShi97/FlowFormerPlusPlus`

[2] `https://github.com/autonomousvision/unimatch`

[3] `https://www.cns.nyu.edu/~lcv/MTmodel/`

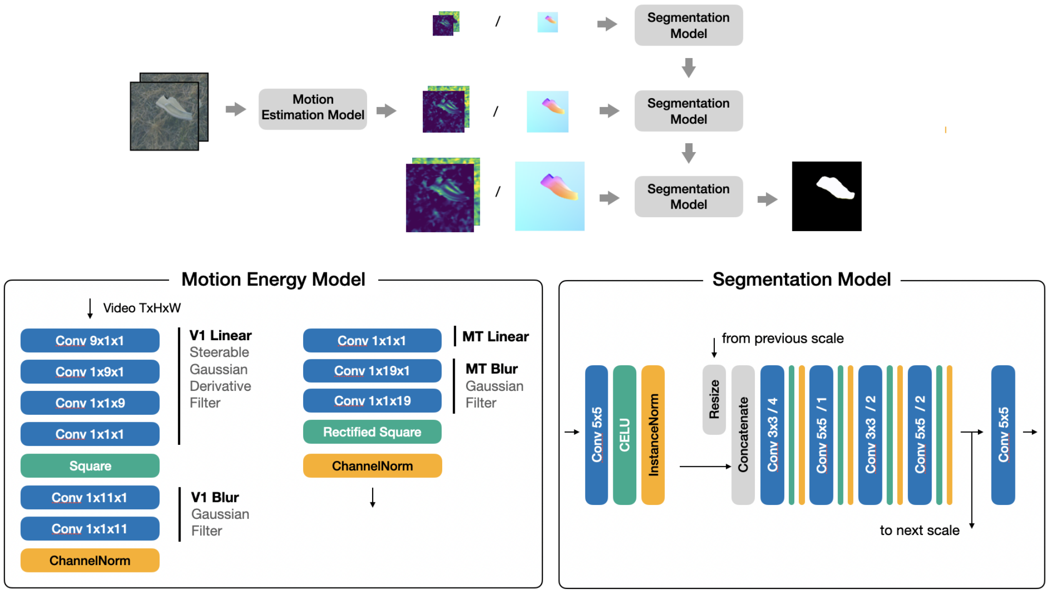

Figure 2: (*top*) Our motion segmentation architecture: The motion estimation predicts multi-scale optical flow or motion energy, the segmentation model predicts the moving foreground region. (*bottom left*) The motion energy model is implemented as a CNN. The weights are chosen such that the CNN is equivalent to the original model by [37]. (*bottom right*) The segmentation model combines motion features across scale and predicts a binary segmentation at the input resolution.

backgrounds used for dataset generation are scans of everyday objects and scenes, resulting in highly realistic renderings. We used 901 videos for training and 100 test videos, each having 90 frames at 30Hz. The training and test videos used different sets of object and backgrounds but are otherwise sampled from the same distribution. The code and hyperparameters for generating videos, as well as the rendered dataset, are publicly available[4].

For all models, we freeze the weights of the motion estimator and only train the downstream segmentation network. As common for binary motion segmentation, we use per pixel binary cross entropy to the ground truth masks as loss. We use the Adam optimizer [21] with a learning rate of $1e-4$ for all models and train for 40.000 steps using a batch size of 8. All models are trained on NVIDIA GeForce RTX 2080 Ti GPUs with 12GB of VRAM. Depending on the computational requirements of the motion model, training the segmentation model on a single GPU takes between 2 and 6 hours.

3.5 Zero-shot evaluation on random dot stimuli

We evaluate models on the original test videos as well as random dot stimuli generated for all test videos based on the ground truth optical flow. We use the same procedure as [31] for generating random dot stimuli using 500 dots with a lifetime of 8 frames, which matches the dot density and lifetimes.

We apply all models using a shifting window approach for the full length videos, but excluding the first and last four frames so that the window is fully contained within the video for all models. For evaluation, we obtain a binary prediction by thresholding with 0.5 and measure performance by computing IoU and F-Score for each frame individually and then averaging over the test set.

[4] https://github.com/mtangemann/motion_energy_segmentation

4 Results

4.1 Zero-Shot Random Dot Segmentation

Table 1 summarizes the motion segmentation performances achieved when using different motion estimators, both on the i.i.d. test set and the corresponding random dot stimuli. For a better overview, we visualize the performances as measured by IoU in Figure 1 and in the appendix.

		Original		Random Dots	
Motion Estimator	Training Dataset	IoU	F-Score	IoU	F-Score
Motion Energy (ours)	-	0.759	0.845	**0.600**	**0.718**
GMFlow	Flying Things 3D	0.885	0.925	0.381	0.493
(2 scales, 6 refinements)	Sintel	0.823	0.874	0.222	0.315
	Mixed	0.823	0.874	0.069	0.106
FlowNet2 SD	FlyingChairs	0.828	0.884	0.377	0.499
FlowNet2 CSS	FlyingThings3D	0.837	0.896	0.351	0.469
	FlyingChairs	0.735	0.818	0.252	0.359
PWC-Net	FlyingThings3D	0.729	0.815	0.347	0.469
	FlyingChairs	0.544	0.662	0.324	0.442
	KITTI	0.600	0.715	0.121	0.193
FlowNet2	FlyingChairs	0.662	0.757	0.278	0.380
	FlyingThings3D	0.821	0.877	0.154	0.241
FlowNet2 CS	FlyingThings3D	0.800	0.867	0.269	0.374
	FlyingChairs	0.669	0.760	0.247	0.359
GMFlow (2 scales)	Flying Things 3D	0.704	0.793	0.267	0.373
	Sintel	0.733	0.812	0.253	0.351
	Mixed	0.743	0.822	0.210	0.300
GMFlow (1 scale)	Mixed	0.843	0.897	0.225	0.308
	Flying Things 3D	0.797	0.859	0.174	0.244
GMA (+P)	KITTI	0.520	0.630	0.154	0.224
	FlyingChairs	0.646	0.717	0.101	0.142
	Mixed	0.895	0.932	0.054	0.078
	FlyingThings3D	0.850	0.894	0.039	0.057
FlowFormer++	Flying Chairs	0.741	0.800	0.144	0.218
	Flying Things 3D	0.901	0.935	0.119	0.182
	Sintel	**0.908**	**0.942**	0.092	0.140
	Flying Things 3D	0.902	0.938	0.072	0.113
GMA	KITTI	0.579	0.679	0.143	0.214
	FlyingChairs	0.643	0.724	0.134	0.194
	FlyingThings3D	0.867	0.909	0.100	0.150
	FlyingThings3D + Sintel	0.890	0.928	0.089	0.132
	Mixed	0.890	0.927	0.077	0.109
GMA (P-only)	FlyingChairs	0.663	0.743	0.138	0.207
	KITTI	0.567	0.650	0.112	0.159
	Mixed	0.881	0.920	0.093	0.141
	FlyingThings3D	0.867	0.909	0.090	0.142
RAFT	FlyingThings3D + Sintel	0.886	0.924	0.132	0.180
	FlyingThings3D	0.869	0.909	0.116	0.172
	Mixed	0.885	0.925	0.108	0.145
	KITTI	0.506	0.600	0.107	0.147
	FlyingChairs	0.647	0.718	0.100	0.147

Table 1: Model performances for the i.i.d. test videos and zero shot to the corresponding random dot stimuli with the same motion patterns. For all motion estimators, the same segmentation network is used to predict the figure-ground segmentation. Results are grouped by the motion estimation model and ordered by the performance on the random dot stimuli.

Recent optical flow methods perform strongly on the original videos. FlowFormer++ works best on our dataset with an IoU of 90.8%, closely followed by a GMA variant that reaches 89.5% IoU.

These results parallel the strong performance of recent Transformer-based architectures on standard optical flow benchmarks. The motion energy based model only achieves a performance of 75.9% IoU and lags behind state-of-the-art optical flow models, but performs similar as earlier deep learning based optical flow models. This result is remarkable when considering that the motion energy model predates the deep learning models by several decades and has not been tuned for dense, end-to-end motion prediction. Within each model, the checkpoints from the FlyingThings3d dataset tend to perform best for the original videos. The FlyingThings3d dataset contains renderings of 3D objects undergoing rigid motion, so arguably it is the most similar dataset compared to the one used in this study.

Motion energy generalizes much better to random dots. The motion energy based model reaches an IoU of 60.0%, which outperforms the performance of the second best model by more than 20 percentage points. Strikingly, the FlowFormer++ and GMA models that performed best on the original videos generalize particularly bad to the random dot stimli (IoU < 10%). Overall, more dated optical flow architectures such as FlowNet2 variants and PWC-Net tend to generalize better to random dot stimuli than more recent approaches. An interesting exception is GMFlow, which reached an IoU of 38.1% and performed best among all optical flow models. We do not observe a clear effect of the training dataset.

We visualize model predictions in Figure 3. For the original videos, the quality of the predicted optical flow varies but allows for a clear segmentation of the moving object. The object is also clearly represented in the motion energy maps, with some feature maps responding highly to the background and others to the moving object. The motion energy maps however tend to be noisier than the optical flow predictions, which explains the lower performance of the motion energy model for the clean videos.

The random dot stimuli exhibits the same motion as the original video, so the prediction of an ideal motion estimator would be unchanged. The optical flow methods however fail to properly estimate the motion of the foreground object. While some methods like FlowNet 2.0 and PWC-Net predict a highly noisy motion pattern that roughly matches the location of the foreground object, many optical flow estimators fail to detect the foreground motion at all. The motion energy on the other hand looks highly similar for the random dot stimulus and the original video, allowing the motion energy segmentation to generalize well in this case.

4.2 Ablation study

As an ablation study, we evaluated whether the performance of the motion energy segmentation model can be improved by learning the parameters of the motion model. We tested different combinations of layers in the motion energy CNN that are fixed, finetuned or trained from scratch and trained them end-to-end with the segmentation model.

The results in table 2 show that the original weights of the model allow for the best generalization to random dots. This is remarkable when considering that the weights of the motion energy model have been originally selected to explain the tuning properties of individual neurons, but not for image-computable motion estimation. Some of the configurations however outperformed the original weights on the original videos. So while the network architecture allows for generalization in principle, all our models trained by gradient descent converged to solutions that performed well on the training data but did not generalize.

As a further ablation study, we removed or replaced layers of the motion energy model. The results in the supplemental information suggest that the pooling and normalization layers are particularly important for generalization to random dots. More details and further experiments are provided in the supplemental information.

5 Human Machine Comparison

The previous results have revealed differences between different motion estimation models in terms of generalization to random dots. While it is known that humans can recognize objects in random dot stimuli without prior training [31], the ability to segment objects in moving random dot patterns has not been quantified before. We therefore conduct a human subject study in order to directly compare the zero-shot generalization to random dots in humans and machines.

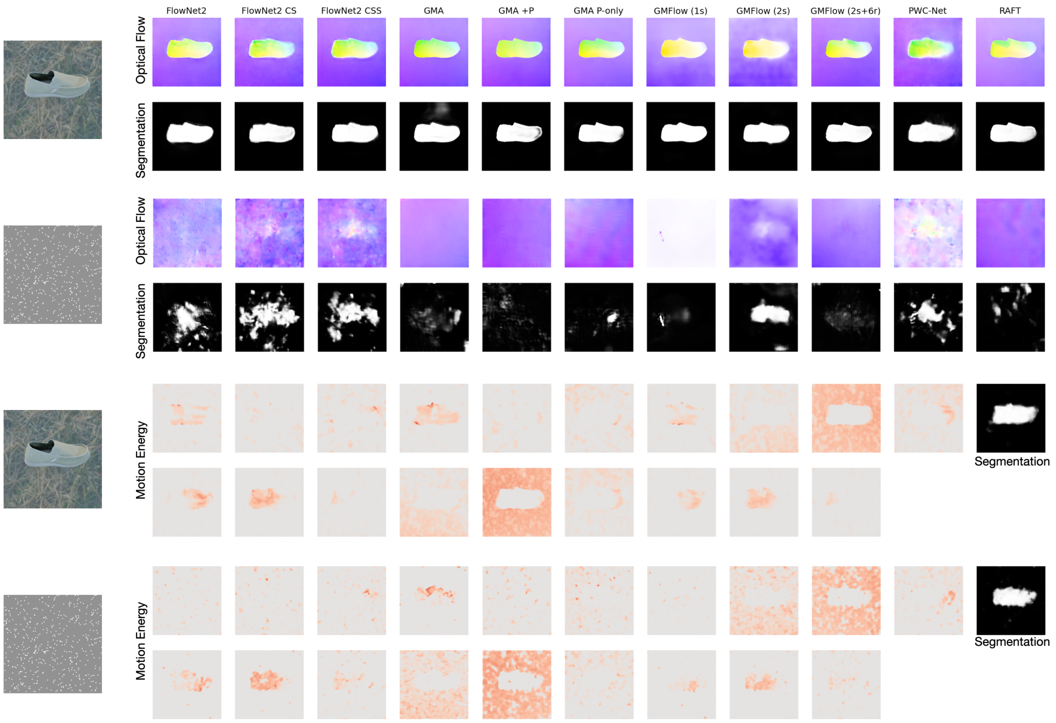

Figure 3: Example predictions for different motion estimators. The motion pattern in the random dot stimulus is the same as in the original video. While the optical flow estimates are highly accurate for the original videos, the models struggle with the random dot stimuli that exhibit the same motion. The activations of the motion energy model model however generalize well to the random dot stimuli, enabling to detect and segment the foreground object.

				Original		Random Dots	
V1 Linear	V1 Blur	MT Linear	MT Blur	IoU	F-Score	IoU	F-Score
fix	fix	fix	fix	0.759	0.845	**0.600**	**0.718**
fix	fix	finetune	fix	0.776	0.856	0.563	0.686
finetune	fix	finetune	fix	0.804	0.873	0.468	0.599
fix	fix	scratch	scratch	0.794	0.873	0.463	0.583
finetune	fix	scratch	scratch	**0.827**	**0.887**	0.395	0.508
finetune	finetune	scratch	cratch	0.600	0.717	0.162	0.246
scratch	fix	scratch	fix	0.660	0.752	0.052	0.087
scratch	scratch	scratch	scratch	0.593	0.702	0.027	0.048

Table 2: Comparison of using the original weights (fix), finetuning the original weights (finetung) or training from scratch (scratch) for the layers of the motion energy model.

Due to the inherent difficulty in directly evaluating the segmentation perceived by humans, we employed a shape identification task as a surrogate requiring segmentation (Figure 4). Each trial involved a random target shape and a distractor shape from the Infinite dSprites dataset [12]. The random dot stimulus shows the target shape moving linearly across the center of the image with random motion direction and speed. After the video concluded, participants were shown clean renderings of the target and distractor shapes and were required to select the shape that they perceived in the random dot stimulus. Since the shape alternatives were unknown while the random dot stimulus was shown, participants had to segment and memorize the shape in the random dot video and then compare it to the shape choices afterward. Therefore, performing well on this task necessitates sufficiently good segmentation of the moving shapes within the motion patterns of the random dot stimuli.

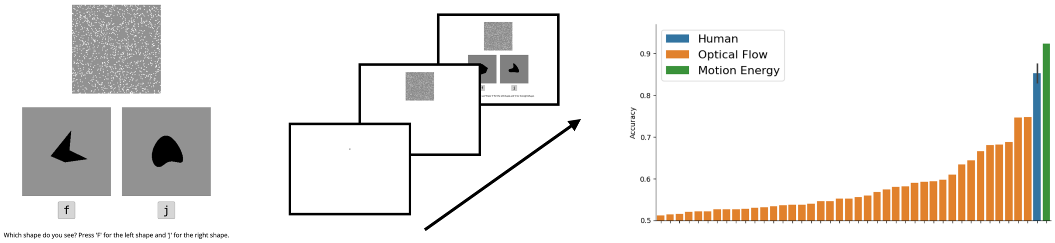

Figure 4: We compare humans and machines using a *random dot shape identification* task as a proxy to measure segmentation in humans. Shown a video of random dots, participants have to respond which of two shapes was perceived in the video. Humans outperformed all optical flow based models, but not the motion energy based model for this task. More details are provided in the supplemental material.

We performed the study in a controlled vision lab environment, where participants viewed the experiment on a VIEWPixx 3D LCD monitor (1920x1080, 120Hz) with the distance fixed to 65cm using a chin rest. The duration of all videos was 1s at a framerate of 30 Hz. Overall, we collected data from N=13 subjects, of which we excluded one subject due to insufficient visual acuity (remaining: N=12, 4 female, 8 male). Among the subjects where both trained vision scientists and naive subjects.

We evaluated all models on the same stimuli as human subjects. Given a random dot video, we applied the respective model to segment the video and selected the shape option that better matched the prediction as measured by IoU.

The results in Figure 4 show that all models based on optical flow are clearly outperformed by humans. Many of the optical flow based models perform near chance level, while some models reached a non-trivial performance. Overall, more recent optical flow models that perform very well on the original videos appear to generalize worse to this task, with GMFlow [53, 54] being a noteable exception. Different from the optical flow models, the motion energy based approach is the only model to match and even outperform human performance. More detailed results in the supplemental information show that the motion energy segmentation model performs on par with the highest performing participants of the study.

6 Limitations

To allow for comparing a large number of motion estimation models with a reasonable computational budget we made compromises for other modeling aspects. We limited the size of the segmentation network to allow for efficient training but performed a control experiment to show that using a more sophisticated segmentation network does not improve generalization (see supplemental information). Moreover, we used the same training schedule for all models but ensured that our setting supports all models adequately by visually inspecting the loss curves.

When comparing humans and machines we did not model several factors that are expected to influence human performance, such as the impact of internal noise and attentional lapses. As common in psychophysics experiments, several subjects reported making accidental errors for few examples [50] which negatively affects performance. So even a model that perfectly replicates the motion processing algorithm in humans is not expected to perfectly replicate human behavior in our setting.

7 Broader impact

This work is highly interdisciplinary, bridging state-of-the-art computer vision motion segmentation algorithms with the principles of Gestalt psychology and the neuroscience of cortical motion processing in the brain. By showing that a neuroscience-inspired motion energy model can outperform conventional optical flow models in zero-shot generalization to random dot stimuli, the study highlights the potential for integrating biological insights into AI systems. Benefits of broader impact include the development of more robust and human-like AI systems, educational value, and the creation of AI systems that are more aligned with human cognition.

8 Discussion

Computational models for motion estimation have a long history in both computational neuroscience and computer vision. Shallow models based on spatio-temporal filtering in pixel space have been able to predict neural activity in brain areas related to motion perception [37, 32] and are compatible with a range of phenomena in human perception [57]. In computer vision, models based on matching deep features between two frames have continuously improved performance over the last years and are successfully applied in a range of downstream tasks. Despite these successes, our study reveals a striking gap between deep optical flow networks and human perception: While humans generalize the common fate Gestalt principle to zero-shot segmentation of random moving dots, the optical flow models fail to generalize to these stimuli. Furthermore, we show that a classic motion energy approach can be scaled to realistic videos while matching human generalization capabilities.

The great success of deep neural networks in computer vision has spawned interest in using DNNs also as a model for human vision, in particular for core object recognition [55]. In the same spirit, deep neural networks might be promising models for human motion perception [56]. While promising, our study parallels findings for core object recognition that show striking differences between human perception and DNNs [49]. For motion perception, however, we show that is possible to combine classical models from computational neuroscience with the scalability of deep learning. Further integration of these modeling traditions is a promising path towards image computable models of human motion perception [41].

While closing the gap between human perception and machine vision is crucial for computational neuroscience, we believe that computer vision likely profits from better alignment with human vision as well. Humans still greatly outperform machines in terms of robustness and efficiency. Our study suggests a substantial entanglement of motion estimation with appearance in DNNs, which might also be linked to the lack of robustness observed in state-of-the-art motion estimators [33, 34]. Computational principles that better match human vision should be considered as promising candidates for addressing these issues.

Finally, we argue that deep learning based models as presented in our work have the potential to greatly improve our understanding of motion perception in humans. Low-level mechanisms for motion estimation and higher level processes for motion interpretation have been mostly studied in isolation [27]. In our work we follow a more holistic approach by studying the effects motion detection mechanisms on the perception of moving objects, which offers several unique opportunities. First, it is not necessary for most downstream tasks to perfectly estimate the physically correct motion. For example, segmenting moving objects does require precise information about object boundaries while other mistakes are less critical. Studying motion estimation and interpretation jointly allows to better understand viable compromises in estimation accuracy as the basis for more efficient processing. Second, studying end-to-end models of motion estimation and interpretation advances our understanding of how neural mechanisms give rise to behavior. DNNs are a particularly promising modeling approach positioned in a “Goldilocks zone” regarding the trade-off between biological plausibility and scalability to natural stimuli and tasks [10]. In this vein, our work establishes a compelling link between cortical mechanisms for motion estimation and the Gestalt psychology of human object perception.

In the future, this work can be extended in several directions. While scaling remarkably well, the original motion energy model is not able to match the performance of state-of-the-art optical flow methods on natural scenes. We see integrating principles from computational neuroscience with techniques from deep learning as a promising path towards closing this gap [41]. Moreover, training the parameters of the CNN implementation of the motion energy model jointly with the segmentation model did not lead to a generalizable solution. How humans learn generalizable motion perception from data, or to which degree this capability is innate, are important questions for future research. Finally, in the spirit of the neuroconnectionist research programme [10] we see our model as an executable hypothesis for motion perception in the human brain. While matching human performance in terms of generalization to moving random dots, this model might well fail to capture other aspects of human motion perception. Further evaluating and extending models of motion perception to capture a diverse range of phenomena is an exciting path towards a holistic understanding of human perception.

Acknowledgments and Disclosure of Funding

This work was supported by the German Research Foundation (DFG): SFB 1233, Robust Vision: Inference Principles and Neural Mechanisms, TP 4, project number: 276693517. The authors thank the International Max Planck Research School for Intelligent Systems for supporting MT. We thank Felix Wichmann, Thomas Klein and all other members of the Wichmann-Lab for supporting and testing the human machine comparison study, and Larissa Höfling for valuable feedback on the manuscript.

References

[1] E. H. Adelson and J. R. Bergen. Spatiotemporal energy models for the perception of motion. *Journal of the Optical Society of America A*, 2(2):284–299, February 1985. doi: 10.1364/JOSAA.2.000284.

[2] E. H. Adelson and J. A. Movshon. Phenomenal coherence of moving visual patterns. *Nature*, 300(5892):523–525, December 1982. doi: 10.1038/300523a0.

[3] J. T. Barron. Continuously Differentiable Exponential Linear Units. *arXiv preprint arXiv:1704.07483*, April 2017. doi: 10.48550/arXiv.1704.07483.

[4] P. Bideau and E. Learned-Miller. It's Moving! A Probabilistic Model for Causal Motion Segmentation in Moving Camera Videos. In *Computer Vision – ECCV 2016*, pages 433–449, Cham, October 2016. Springer International Publishing. doi: 10.1007/978-3-319-46484-8_26.

[5] P. Bideau, A. RoyChowdhury, R. R. Menon, and E. Learned-Miller. The Best of Both Worlds: Combining CNNs and Geometric Constraints for Hierarchical Motion Segmentation. In *Proceedings of the IEEE Conference on Computer Vision and Pattern Recognition (CVPR)*, pages 508–517, June 2018.

[6] T. Brox and J. Malik. Object Segmentation by Long Term Analysis of Point Trajectories. In *Computer Vision – ECCV 2010*, volume 6315 of *Lecture Notes in Computer Science*, pages 282–295, Berlin, Heidelberg, September 2010. Springer. doi: 10.1007/978-3-642-15555-0_21.

[7] D. J. Butler, J. Wulff, G. B. Stanley, and M. J. Black. A Naturalistic Open Source Movie for Optical Flow Evaluation. In *Computer Vision – ECCV 2012*, volume 7577 of *Lecture Notes in Computer Science*, pages 611–625, Berlin, Heidelberg, October 2012. Springer. doi: 10.1007/978-3-642-33783-3_44.

[8] M. Contributors. MMFlow: OpenMMLab Optical Flow Toolbox and Benchmark, 2021.

[9] A. Dave, P. Tokmakov, and D. Ramanan. Towards Segmenting Anything That Moves. In *Proceedings of the IEEE/CVF International Conference on Computer Vision (ICCV) Workshops*, October 2019.

[10] A. Doerig, R. P. Sommers, K. Seeliger, B. Richards, J. Ismael, G. W. Lindsay, K. P. Kording, T. Konkle, M. A. J. van Gerven, N. Kriegeskorte, and T. C. Kietzmann. The neuroconnectionist research programme. *Nature Reviews Neuroscience*, 24(7):431–450, July 2023. doi: 10.1038/s41583-023-00705-w.

[11] A. Dosovitskiy, P. Fischer, E. Ilg, P. Hausser, C. Hazirbas, V. Golkov, P. van der Smagt, D. Cremers, and T. Brox. FlowNet: Learning Optical Flow With Convolutional Networks. In *Proceedings of the IEEE International Conference on Computer Vision (ICCV)*, pages 2758–2766, December 2015.

[12] S. Dziadzio, Ç. Yıldız, G. M. van de Ven, T. Trzciński, T. Tuytelaars, and M. Bethge. Infinite dSprites for Disentangled Continual Learning: Separating Memory Edits from Generalization. In *3rd Conference on Lifelong Learning Agents (CoLLAs)*, July 2024.

[13] C. L. Fennema and W. B. Thompson. Velocity determination in scenes containing several moving objects. *Computer Graphics and Image Processing*, 9(4):301–315, April 1979. doi: 10.1016/0146-664X(79)90097-2.

[14] K. Greff, F. Belletti, L. Beyer, C. Doersch, Y. Du, D. Duckworth, D. J. Fleet, D. Gnanapragasam, F. Golemo, C. Herrmann, T. Kipf, A. Kundu, D. Lagun, I. Laradji, H.-T. D. Liu, H. Meyer, Y. Miao, D. Nowrouzezahrai, C. Oztireli, E. Pot, N. Radwan, D. Rebain, S. Sabour, M. S. M. Sajjadi, M. Sela, V. Sitzmann, A. Stone, D. Sun, S. Vora, Z. Wang, T. Wu, K. M. Yi, F. Zhong, and A. Tagliasacchi. Kubric: A Scalable Dataset Generator. In *Proceedings of the IEEE/CVF Conference on Computer Vision and Pattern Recognition (CVPR)*, pages 3749–3761, June 2022.

[15] D. J. Heeger, E. P. Simoncelli, and J. A. Movshon. Computational models of cortical visual processing. *Proceedings of the National Academy of Sciences*, 93(2):623–627, January 1996. doi: 10.1073/pnas.93.2.623.

[16] B. K. P. Horn and B. G. Schunck. Determining optical flow. *Artificial Intelligence*, 17(1): 185–203, August 1981. doi: 10.1016/0004-3702(81)90024-2.

[17] E. Ilg, N. Mayer, T. Saikia, M. Keuper, A. Dosovitskiy, and T. Brox. FlowNet 2.0: Evolution of Optical Flow Estimation With Deep Networks. In *Proceedings of the IEEE Conference on Computer Vision and Pattern Recognition (CVPR)*, pages 2462–2470, July 2017.

[18] S. Jiang, D. Campbell, Y. Lu, H. Li, and R. Hartley. Learning To Estimate Hidden Motions With Global Motion Aggregation. In *Proceedings of the IEEE/CVF International Conference on Computer Vision (ICCV)*, pages 9772–9781, October 2021.

[19] G. Johansson. Visual perception of biological motion and a model for its analysis. *Perception & Psychophysics*, 14(2):201–211, June 1973. doi: 10.3758/BF03212378.

[20] M. Keuper, B. Andres, and T. Brox. Motion Trajectory Segmentation via Minimum Cost Multicuts. In *Proceedings of the IEEE International Conference on Computer Vision (ICCV)*, pages 3271–3279, December 2015.

[21] D. P. Kingma and J. Ba. Adam: A Method for Stochastic Optimization. In *3rd International Conference on Learning Representations (ICLR) 2015*. arXiv, May 2015. doi: 10.48550/arXiv.1412.6980.

[22] H. Lamdouar, C. Yang, W. Xie, and A. Zisserman. Betrayed by Motion: Camouflaged Object Discovery via Motion Segmentation. In *Proceedings of the Asian Conference on Computer Vision (ACCV)*, November 2020.

[23] H. Lamdouar, W. Xie, and A. Zisserman. Segmenting Invisible Moving Objects. In *32nd British Machine Vision Conference (BMVC)*, November 2021.

[24] N. Mayer, E. Ilg, P. Hausser, P. Fischer, D. Cremers, A. Dosovitskiy, and T. Brox. A Large Dataset to Train Convolutional Networks for Disparity, Optical Flow, and Scene Flow Estimation. In *Proceedings of the IEEE Conference on Computer Vision and Pattern Recognition (CVPR)*, pages 4040–4048, June 2016.

[25] M. Menze, C. Heipke, and A. Geiger. JOINT 3D ESTIMATION OF VEHICLES AND SCENE FLOW. *ISPRS Annals of the Photogrammetry, Remote Sensing and Spatial Information Sciences*, II-3/W5:427–434, September 2015. doi: 10.5194/isprsannals-II-3-W5-427-2015.

[26] M. Menze, C. Heipke, and A. Geiger. Object Scene Flow. *ISPRS Journal of Photogrammetry and Remote Sensing*, 140:60–76, June 2018. doi: 10.1016/j.isprsjprs.2017.09.013.

[27] S. Nishida, T. Kawabe, M. Sawayama, and T. Fukiage. Motion Perception: From Detection to Interpretation. *Annual Review of Vision Science*, 4(1):501–523, September 2018. doi: 10.1146/annurev-vision-091517-034328.

[28] S. Nishimoto, A. T. Vu, T. Naselaris, Y. Benjamini, B. Yu, and J. L. Gallant. Reconstructing Visual Experiences from Brain Activity Evoked by Natural Movies. *Current Biology*, 21(19): 1641–1646, October 2011. doi: 10.1016/j.cub.2011.08.031.

[29] P. Ochs and T. Brox. Object segmentation in video: A hierarchical variational approach for turning point trajectories into dense regions. In *2011 International Conference on Computer Vision*, pages 1583–1590, November 2011. doi: 10.1109/ICCV.2011.6126418.

[30] A. Paszke, S. Gross, F. Massa, A. Lerer, J. Bradbury, G. Chanan, T. Killeen, Z. Lin, N. Gimelshein, L. Antiga, A. Desmaison, A. Kopf, E. Yang, Z. DeVito, M. Raison, A. Tejani, S. Chilamkurthy, B. Steiner, L. Fang, J. Bai, and S. Chintala. PyTorch: An Imperative Style, High-Performance Deep Learning Library. In *Advances in Neural Information Processing Systems*, volume 32. Curran Associates, Inc., December 2019.

[31] S. Robert, L. G. Ungerleider, and M. Vaziri-Pashkam. Disentangling Object Category Representations Driven by Dynamic and Static Visual Input. *Journal of Neuroscience*, 43(4):621–634, January 2023. doi: 10.1523/JNEUROSCI.0371-22.2022.

[32] N. C. Rust, V. Mante, E. P. Simoncelli, and J. A. Movshon. How MT cells analyze the motion of visual patterns. *Nature Neuroscience*, 9(11):1421–1431, November 2006. doi: 10.1038/nn1786.

[33] J. Schmalfuss, L. Mehl, and A. Bruhn. Attacking Motion Estimation with Adversarial Snow. In *ECCV 2022 Workshop on Adversarial Robustness in the Real World*, October 2022.

[34] J. Schmalfuss, P. Scholze, and A. Bruhn. A Perturbation-Constrained Adversarial Attack for Evaluating the Robustness of Optical Flow. In *Computer Vision – ECCV 2022*, pages 183–200, Cham, October 2022. Springer Nature Switzerland. doi: 10.1007/978-3-031-20047-2_11.

[35] H. H. Schütt, S. Harmeling, J. H. Macke, and F. A. Wichmann. Painfree and accurate Bayesian estimation of psychometric functions for (potentially) overdispersed data. *Vision Research*, 122: 105–123, May 2016. doi: 10.1016/j.visres.2016.02.002.

[36] X. Shi, Z. Huang, D. Li, M. Zhang, K. C. Cheung, S. See, H. Qin, J. Dai, and H. Li. FlowFormer++: Masked Cost Volume Autoencoding for Pretraining Optical Flow Estimation. In *Proceedings of the IEEE/CVF Conference on Computer Vision and Pattern Recognition (CVPR)*, pages 1599–1610, June 2023.

[37] E. P. Simoncelli and D. J. Heeger. A model of neuronal responses in visual area MT. *Vision Research*, 38(5):743–761, March 1998. doi: 10.1016/S0042-6989(97)00183-1.

[38] F. Solari, M. Chessa, N. V. K. Medathati, and P. Kornprobst. What can we expect from a V1-MT feedforward architecture for optical flow estimation? *Signal Processing: Image Communication*, 39:342–354, November 2015. doi: 10.1016/j.image.2015.04.006.

[39] D. Sun, X. Yang, M.-Y. Liu, and J. Kautz. PWC-Net: CNNs for Optical Flow Using Pyramid, Warping, and Cost Volume. In *Proceedings of the IEEE Conference on Computer Vision and Pattern Recognition (CVPR)*, pages 8934–8943, June 2018.

[40] D. Sun, X. Yang, M.-Y. Liu, and J. Kautz. Models Matter, So Does Training: An Empirical Study of CNNs for Optical Flow Estimation. *IEEE Transactions on Pattern Analysis and Machine Intelligence*, 42(6):1408–1423, June 2020. doi: 10.1109/TPAMI.2019.2894353.

[41] Z. Sun, Y.-J. Chen, Y.-H. Yang, and S. Nishida. Modeling Human Visual Motion Processing with Trainable Motion Energy Sensing and a Self-attention Network. In *Advances in Neural Information Processing Systems*, volume 36, pages 24335–24348. Curran Associates, Inc., December 2023.

[42] M. Tangemann, S. Schneider, J. von Kügelgen, F. Locatello, P. V. Gehler, T. Brox, M. Kümmerer, M. Bethge, and B. Schölkopf. Unsupervised Object Learning via Common Fate. In *Proceedings of the Second Conference on Causal Learning and Reasoning*, pages 281–327. PMLR, April 2023.

[43] Z. Teed and J. Deng. RAFT: Recurrent All-Pairs Field Transforms for Optical Flow. In *Computer Vision – ECCV 2020*, pages 402–419, Cham, August 2020. Springer International Publishing. doi: 10.1007/978-3-030-58536-5_24.

[44] P. Tokmakov, C. Schmid, and K. Alahari. Learning to Segment Moving Objects. *International Journal of Computer Vision*, 127(3):282–301, March 2019. doi: 10.1007/s11263-018-1122-2.

[45] D. Ulyanov, A. Vedaldi, and V. Lempitsky. Instance Normalization: The Missing Ingredient for Fast Stylization. *arXiv preprint arXiv:1607.08022*, November 2017. doi: 10.48550/arXiv.1607.08022.

[46] A. B. Watson and A. J. Ahumada. Model of human visual-motion sensing. *Journal of the Optical Society of America A*, 2(2):322–342, February 1985. doi: 10.1364/JOSAA.2.000322.

[47] M. Wertheimer. Experimentelle Studien über das Sehen von Bewegung. *Zeitschrift für Psychologie*, 61:161–265, April 1912.

[48] M. Wertheimer. *On Perceived Motion and Figural Organization*. The MIT Press, Cambridge, MA, July 2012.

[49] F. A. Wichmann and R. Geirhos. Are Deep Neural Networks Adequate Behavioral Models of Human Visual Perception? *Annual Review of Vision Science*, 9:501–524, September 2023. doi: 10.1146/annurev-vision-120522-031739.

[50] F. A. Wichmann and N. J. Hill. The psychometric function: I. Fitting, sampling, and goodness of fit. *Perception & Psychophysics*, 63(8):1293–1313, November 2001. doi: 10.3758/BF03194544.

[51] J. Xie, W. Xie, and A. Zisserman. Segmenting Moving Objects via an Object-Centric Layered Representation. In *Advances in Neural Information Processing Systems*, volume 35, pages 28023–28036. Curran Associates, Inc., December 2022.

[52] J. Xie, W. Xie, and A. Zisserman. Appearance-Based Refinement for Object-Centric Motion Segmentation. *arXiv preprint arXiv:2312.11463*, August 2024. doi: 10.48550/arXiv.2312.11463.

[53] H. Xu, J. Zhang, J. Cai, H. Rezatofighi, and D. Tao. GMFlow: Learning Optical Flow via Global Matching. In *Proceedings of the IEEE/CVF Conference on Computer Vision and Pattern Recognition (CVPR)*, pages 8121–8130, June 2022.

[54] H. Xu, J. Zhang, J. Cai, H. Rezatofighi, F. Yu, D. Tao, and A. Geiger. Unifying Flow, Stereo and Depth Estimation. *IEEE Transactions on Pattern Analysis and Machine Intelligence*, 45 (11):13941–13958, November 2023. doi: 10.1109/TPAMI.2023.3298645.

[55] D. L. K. Yamins, H. Hong, C. F. Cadieu, E. A. Solomon, D. Seibert, and J. J. DiCarlo. Performance-optimized hierarchical models predict neural responses in higher visual cortex. *Proceedings of the National Academy of Sciences*, 111(23):8619–8624, May 2014. doi: 10.1073/pnas.1403112111.

[56] Y.-H. Yang, T. Fukiage, Z. Sun, and S. Nishida. Psychophysical measurement of perceived motion flow of naturalistic scenes. *iScience*, 26(12), December 2023. doi: 10.1016/j.isci.2023.108307.

[57] J. Yates. Motion Illusions, December 2020. `https://jake.vision/blog/motion-illusions/` (accessed: 2024-10-24).

Supplemental information

A Additional details about the results

For an additional overview, view visualize the segmentation performances on random dot stimuli as reported in Table 1.

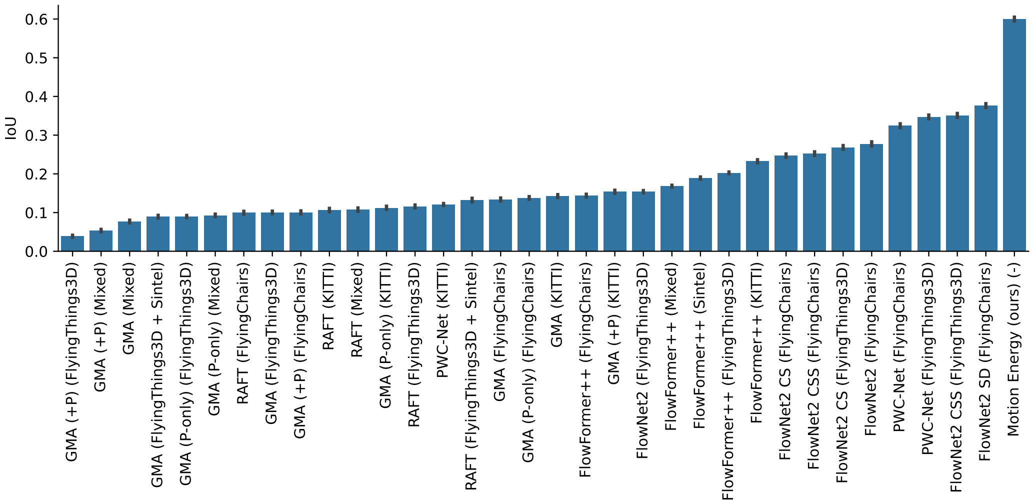

Figure 5: Segmentation performances of the evaluated models on the random dot stimuli. Same data as in Table 1.

B Additional experiments

B.1 Importance of components of the motion energy model

We conducted an additional ablation study in order to better understand which aspects of the motion energy model are essential for generalization to random dot stimuli. We removed or replaced individual layers as described in Table 3 and trained the ablated models from scratch using in the same way as the baseline model.

The results in Table 2 hint at the normalization and pooling layers being important for generalization. When the Gaussian pooling layers are removed completely, the performance on original videos even slightly improves while the generalization to random dot stimuli is substantially reduced.

Replacing the squaring-based nonlinear layers with ReLU layers, however, hardly changes the model's performance.

Condition	Original IoU ↑	 F-Score ↑	Random Dots IoU ↑	 F-Score ↑
Baseline	0.759	0.845	0.600	0.718
Replace RectifiedSquare → ReLU (MT)	0.753	0.838	**0.609**	**0.725**
Replace Square → ReLU (V1)	0.770	0.854	0.536	0.663
Remove MT Linear	0.768	0.856	0.481	0.609
Remove MT	0.770	0.854	0.451	0.583
Remove Blur (V1, MT)	**0.801**	**0.872**	0.421	0.540
Replace ChannelNorm → InstanceNorm (V1, MT)	0.592	0.703	0.230	0.340
Remove Normalization (V1, MT)	0.400	0.516	0.018	0.018

Table 3: Ablation study: Performance of the model on original videos and corresponding random dot stimuli with various layers of the motion energy model removed or replaced. Results are ordered by IoU on the random dot stimuli.

B.2 Multi-frame optical flow

The motion energy model uses a window of 9 frames as input, while typical optical flow methods estimate correspondences between only two frames. To rule out the possibility that the results observed in our paper are mainly explained by the different input window lengths, we perform an ablation study in which we apply optical flow methods using the same 9 frame windows. For each window, we compute the optical flow between the central frame, for which the segmentation has to be predicted, to the 8 other frames in the window. The stacked optical flow fields are then used as the input to the segmentation network.

The results in Table 4 and Figure 6 show some improvement on the original videos but an ever wider gap to the motion energy model in terms of of generalization to random dots. The differences between the motion energy and optical flow models therefore cannot be explained by the different input lengths.

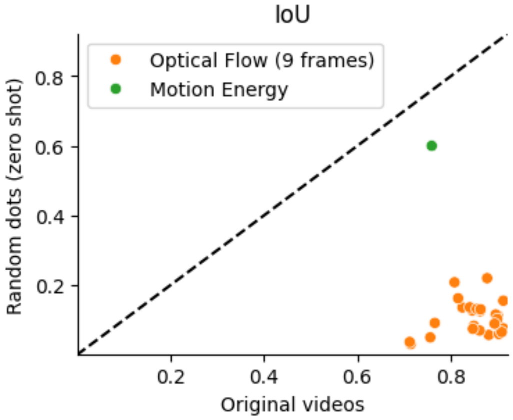

Figure 6: Performance of multi-frame optical flow based models on the original videos and corresponding random dot videos.

B.3 Comparison with state-of-the-art motion segmentation

In our study we used a relatively small segmentation network downstream to the respective motion estimator. State-of-the-art motion segmentation models typically target multi-object segmentation in real world videos and therefore use more complex segmentation networks. In order to verify that the results in our paper are not caused by using a smaller segmentation network, we evaluated the state

		Original		Random Dots	
Motion Estimator	Training Dataset	IoU	F-Score	IoU	F-Score
Motion Energy (ours)	-	0.759	0.845	**0.600**	**0.718**
FlowNet2 SD	FlyingChairs	0.878	0.928	0.221	0.325
FlowNet2	FlyingChairs	0.808	0.868	0.209	0.300
	FlyingThings3D	0.881	0.929	0.058	0.100
PWC-Net	FlyingChairs	0.816	0.886	0.163	0.250
	FlyingThings3D	0.825	0.886	0.137	0.221
	KITTI	0.712	0.811	0.038	0.060
RAFT	FlyingThings3D + Sintel	**0.912**	**0.948**	0.156	0.222
	FlyingChairs	0.863	0.914	0.126	0.195
	Mixed	0.896	0.934	0.117	0.164
	FlyingThings3D	0.894	0.934	0.090	0.132
	KITTI	0.714	0.794	0.031	0.053
FlowNet2 CS	FlyingChairs	0.841	0.899	0.137	0.220
	FlyingThings3D	0.847	0.904	0.075	0.129
GMA (+P)	FlyingChairs	0.856	0.912	0.132	0.212
	Mixed	0.900	0.936	0.114	0.179
	FlyingThings3D	0.899	0.936	0.104	0.171
GMA	FlyingChairs	0.864	0.917	0.131	0.212
	Mixed	0.900	0.937	0.090	0.139
	FlyingThings3D + Sintel	0.909	0.943	0.066	0.100
	FlyingThings3D	0.903	0.943	0.060	0.098
	KITTI	0.756	0.834	0.051	0.084
GMA (P-only)	FlyingChairs	0.846	0.901	0.128	0.207
	KITTI	0.766	0.847	0.092	0.155
	FlyingThings3D	0.903	0.940	0.083	0.139
	Mixed	**0.912**	0.947	0.077	0.117
FlowNet2 CSS	FlyingChairs	0.850	0.908	0.084	0.141
	FlyingThings3D	0.862	0.918	0.070	0.121

Table 4: Ablation study: We apply the optical flow estimators to a window of 9 frames by using the central frame as references and computing optical flow to each of the 8 other frames. The stacked optical flow fields are used as inpute for the segmentation network.

of the art OCLR model [51] in our setting. The OCLR model uses optical flow estimated by RAFT [43], which we also included in our experiments. The segmentation network however uses a U-Net architecture with Transformer bottleneck and was trained to segment multiple objects on a synthetic dataset. We use the published weights and do not retrain the model on our data.

The results in Table 5 show that the model performs very well on the original data. OCLR outperforms our motion energy based model and achieves a performance similar to the best optical flow based models considered in this work. At the same time, the model does not generalize to the corresponding random dot stimuli. These results provide further evidence that the low generalization to random dots is not due to the architecture of the segmentation network or the RGB training data, but a property of the motion estimator.

Model	**IoU (original)**	**IoU (random dots)**
OCLR	0.838	0.026
Motion Energy Segmentation	0.759	0.600

Table 5: Comparison of the state-of-the-art motion segmentation model OCLR, and our segmentation model based on a motion energy model.

C Additional details about the human subject study

C.1 Comparison of humans and machines by example difficulty

As a measure of task difficulty, we count the number of *informative dots*. A dot is informative, if it is contained in either the target and distractor shape but not both (see Figure 7, left). Only these dots allow discriminating between the different shapes.

We fitted psychometric curves for human participants and models as a function of the number of informative dots, using the psignifit toolbox [35]. The results in Figure 7 confirm that only the motion energy model is able to match the performance of human subjects, especially for stimuli with a medium number of informative dots.

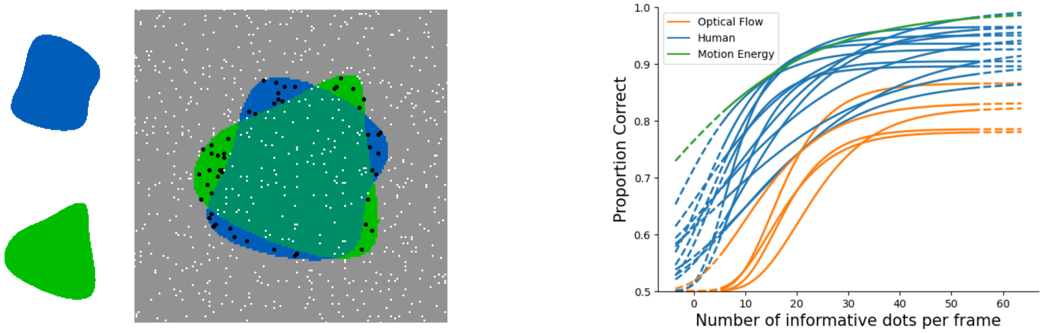

Figure 7: (*left*) As a measure of task difficulty, we count the number of informative dots that allow discriminating betwen the two shape alternatives. (*right*) Psychometric curves for humans, the motion energy based model and the four best optical flow models for the task as in 8.

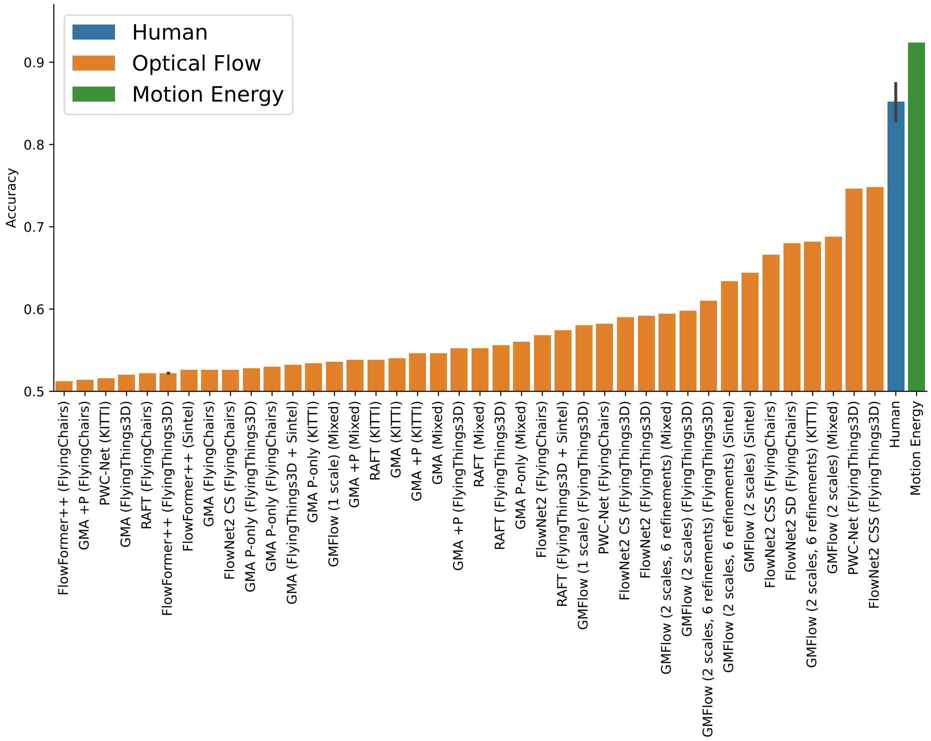

Figure 8: Comparison of the human and model performances for the random dot shape matching task.

C.2 Screenshots of the experiment

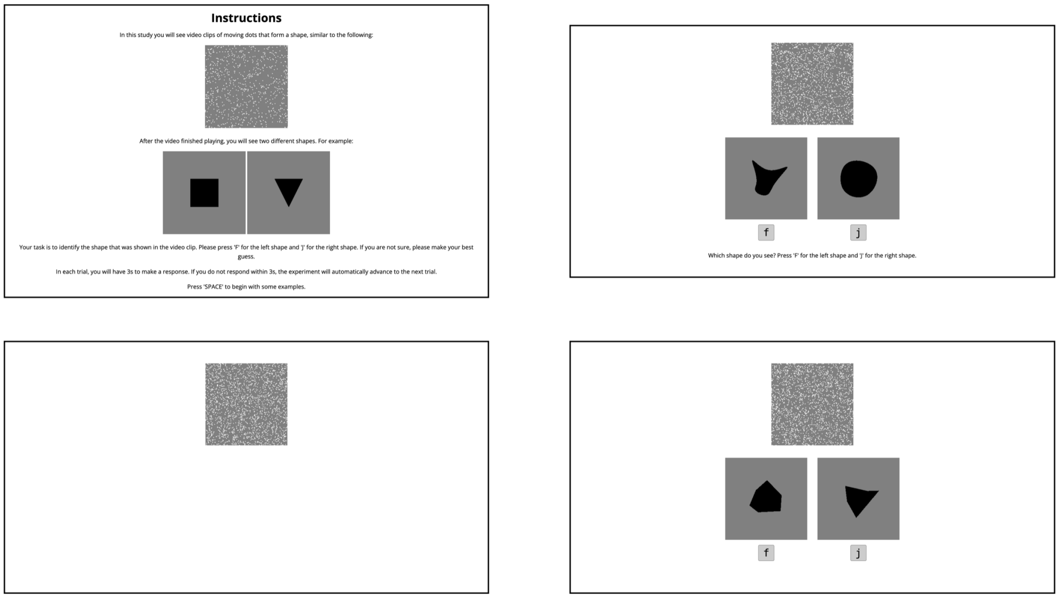

Instructions

In this study you will see video clips of moving dots that form a shape, similar to the following:

After the video finished playing, you will see two different shapes. For example:

Your task is to identify the shape that was shown in the video clip. Please press 'F' for the left shape and 'J' for the right shape. If you are not sure, please make your best guess.

In each trial, you will have 3s to make a response. If you do not respond within 3s, the experiment will automatically advance to the next trial.

Press 'SPACE' to begin with some examples.

Which shape do you see? Press 'F' for the left shape and 'J' for the right shape.

Figure 9: Screenshots from the human subject study on random dot shape identification. (*top left*) Instructions that were shown prior to the experiment. (*top right*) We showed 20 training trials during which subjects could familiarize themselves with the task. (*bottom left*) The training was followed by 500 test trials. A video with the random dot stimuli was shown first. (*bottom right*) Once the video finished playing, the two shape options were shown below.

NeurIPS Paper Checklist

1. **Claims**

   Question: Do the main claims made in the abstract and introduction accurately reflect the paper's contributions and scope?

   Answer: [Yes]

   Justification: We clearly state the main contributions of our work in both the abstract and the introduction. All mentioned results are supported by the experimental data presented in the paper.

   Guidelines:

   - The answer NA means that the abstract and introduction do not include the claims made in the paper.
   - The abstract and/or introduction should clearly state the claims made, including the contributions made in the paper and important assumptions and limitations. A No or NA answer to this question will not be perceived well by the reviewers.
   - The claims made should match theoretical and experimental results, and reflect how much the results can be expected to generalize to other settings.
   - It is fine to include aspirational goals as motivation as long as it is clear that these goals are not attained by the paper.

2. **Limitations**

   Question: Does the paper discuss the limitations of the work performed by the authors?

   Answer: [Yes]

   Justification: The paper includes a separate section that discusses the limitations of our work in detail, including limitations due to computational constraints.

   Guidelines:

   - The answer NA means that the paper has no limitation while the answer No means that the paper has limitations, but those are not discussed in the paper.
   - The authors are encouraged to create a separate "Limitations" section in their paper.
   - The paper should point out any strong assumptions and how robust the results are to violations of these assumptions (e.g., independence assumptions, noiseless settings, model well-specification, asymptotic approximations only holding locally). The authors should reflect on how these assumptions might be violated in practice and what the implications would be.
   - The authors should reflect on the scope of the claims made, e.g., if the approach was only tested on a few datasets or with a few runs. In general, empirical results often depend on implicit assumptions, which should be articulated.
   - The authors should reflect on the factors that influence the performance of the approach. For example, a facial recognition algorithm may perform poorly when image resolution is low or images are taken in low lighting. Or a speech-to-text system might not be used reliably to provide closed captions for online lectures because it fails to handle technical jargon.
   - The authors should discuss the computational efficiency of the proposed algorithms and how they scale with dataset size.
   - If applicable, the authors should discuss possible limitations of their approach to address problems of privacy and fairness.
   - While the authors might fear that complete honesty about limitations might be used by reviewers as grounds for rejection, a worse outcome might be that reviewers discover limitations that aren't acknowledged in the paper. The authors should use their best judgment and recognize that individual actions in favor of transparency play an important role in developing norms that preserve the integrity of the community. Reviewers will be specifically instructed to not penalize honesty concerning limitations.

3. **Theory Assumptions and Proofs**

   Question: For each theoretical result, does the paper provide the full set of assumptions and a complete (and correct) proof?

Answer: [NA]

Justification: The paper does not include theoretical results.

Guidelines:

- The answer NA means that the paper does not include theoretical results.
- All the theorems, formulas, and proofs in the paper should be numbered and cross-referenced.
- All assumptions should be clearly stated or referenced in the statement of any theorems.
- The proofs can either appear in the main paper or the supplemental material, but if they appear in the supplemental material, the authors are encouraged to provide a short proof sketch to provide intuition.
- Inversely, any informal proof provided in the core of the paper should be complemented by formal proofs provided in appendix or supplemental material.
- Theorems and Lemmas that the proof relies upon should be properly referenced.

4. **Experimental Result Reproducibility**

   Question: Does the paper fully disclose all the information needed to reproduce the main experimental results of the paper to the extent that it affects the main claims and/or conclusions of the paper (regardless of whether the code and data are provided or not)?

   Answer: [Yes]

   Justification: We describe the models, data and evaluation protocol used in the paper in detail. Additionally, the code, pretrained models and the contributed dataset are publicly released.

   Guidelines:

   - The answer NA means that the paper does not include experiments.
   - If the paper includes experiments, a No answer to this question will not be perceived well by the reviewers: Making the paper reproducible is important, regardless of whether the code and data are provided or not.
   - If the contribution is a dataset and/or model, the authors should describe the steps taken to make their results reproducible or verifiable.
   - Depending on the contribution, reproducibility can be accomplished in various ways. For example, if the contribution is a novel architecture, describing the architecture fully might suffice, or if the contribution is a specific model and empirical evaluation, it may be necessary to either make it possible for others to replicate the model with the same dataset, or provide access to the model. In general. releasing code and data is often one good way to accomplish this, but reproducibility can also be provided via detailed instructions for how to replicate the results, access to a hosted model (e.g., in the case of a large language model), releasing of a model checkpoint, or other means that are appropriate to the research performed.
   - While NeurIPS does not require releasing code, the conference does require all submissions to provide some reasonable avenue for reproducibility, which may depend on the nature of the contribution. For example
     (a) If the contribution is primarily a new algorithm, the paper should make it clear how to reproduce that algorithm.
     (b) If the contribution is primarily a new model architecture, the paper should describe the architecture clearly and fully.
     (c) If the contribution is a new model (e.g., a large language model), then there should either be a way to access this model for reproducing the results or a way to reproduce the model (e.g., with an open-source dataset or instructions for how to construct the dataset).
     (d) We recognize that reproducibility may be tricky in some cases, in which case authors are welcome to describe the particular way they provide for reproducibility. In the case of closed-source models, it may be that access to the model is limited in some way (e.g., to registered users), but it should be possible for other researchers to have some path to reproducing or verifying the results.

5. **Open access to data and code**

Question: Does the paper provide open access to the data and code, with sufficient instructions to faithfully reproduce the main experimental results, as described in supplemental material?

Answer: [Yes]

Justification: All code and data for the paper is publicly released.

Guidelines:

- The answer NA means that paper does not include experiments requiring code.
- Please see the NeurIPS code and data submission guidelines (`https://nips.cc/public/guides/CodeSubmissionPolicy`) for more details.
- While we encourage the release of code and data, we understand that this might not be possible, so "No" is an acceptable answer. Papers cannot be rejected simply for not including code, unless this is central to the contribution (e.g., for a new open-source benchmark).
- The instructions should contain the exact command and environment needed to run to reproduce the results. See the NeurIPS code and data submission guidelines (`https://nips.cc/public/guides/CodeSubmissionPolicy`) for more details.
- The authors should provide instructions on data access and preparation, including how to access the raw data, preprocessed data, intermediate data, and generated data, etc.
- The authors should provide scripts to reproduce all experimental results for the new proposed method and baselines. If only a subset of experiments are reproducible, they should state which ones are omitted from the script and why.
- At submission time, to preserve anonymity, the authors should release anonymized versions (if applicable).
- Providing as much information as possible in supplemental material (appended to the paper) is recommended, but including URLs to data and code is permitted.

6. **Experimental Setting/Details**

   Question: Does the paper specify all the training and test details (e.g., data splits, hyperparameters, how they were chosen, type of optimizer, etc.) necessary to understand the results?

   Answer: [Yes]

   Justification: Hyperparameters and training details are explicitly reported with the description of the models.

   Guidelines:

   - The answer NA means that the paper does not include experiments.
   - The experimental setting should be presented in the core of the paper to a level of detail that is necessary to appreciate the results and make sense of them.
   - The full details can be provided either with the code, in appendix, or as supplemental material.

7. **Experiment Statistical Significance**

   Question: Does the paper report error bars suitably and correctly defined or other appropriate information about the statistical significance of the experiments?

   Answer: [Yes]

   Justification: Due to space constraints we did not include further statistical information in the main table. However we included a Figure showing the same data with error bars in the supplemental material.

   Guidelines:

   - The answer NA means that the paper does not include experiments.
   - The authors should answer "Yes" if the results are accompanied by error bars, confidence intervals, or statistical significance tests, at least for the experiments that support the main claims of the paper.

- The factors of variability that the error bars are capturing should be clearly stated (for example, train/test split, initialization, random drawing of some parameter, or overall run with given experimental conditions).
- The method for calculating the error bars should be explained (closed form formula, call to a library function, bootstrap, etc.)
- The assumptions made should be given (e.g., Normally distributed errors).
- It should be clear whether the error bar is the standard deviation or the standard error of the mean.
- It is OK to report 1-sigma error bars, but one should state it. The authors should preferably report a 2-sigma error bar than state that they have a 96% CI, if the hypothesis of Normality of errors is not verified.
- For asymmetric distributions, the authors should be careful not to show in tables or figures symmetric error bars that would yield results that are out of range (e.g. negative error rates).
- If error bars are reported in tables or plots, The authors should explain in the text how they were calculated and reference the corresponding figures or tables in the text.

8. **Experiments Compute Resources**

   Question: For each experiment, does the paper provide sufficient information on the computer resources (type of compute workers, memory, time of execution) needed to reproduce the experiments?

   Answer: [Yes]

   Justification: We reported the computational resources of our models with the description of the training details.

   Guidelines:

   - The answer NA means that the paper does not include experiments.
   - The paper should indicate the type of compute workers CPU or GPU, internal cluster, or cloud provider, including relevant memory and storage.
   - The paper should provide the amount of compute required for each of the individual experimental runs as well as estimate the total compute.
   - The paper should disclose whether the full research project required more compute than the experiments reported in the paper (e.g., preliminary or failed experiments that didn't make it into the paper).

9. **Code Of Ethics**

   Question: Does the research conducted in the paper conform, in every respect, with the NeurIPS Code of Ethics `https://neurips.cc/public/EthicsGuidelines`?

   Answer: [Yes]

   Justification: We have read the code of ethics and conform to it in every respect.

   Guidelines:

   - The answer NA means that the authors have not reviewed the NeurIPS Code of Ethics.
   - If the authors answer No, they should explain the special circumstances that require a deviation from the Code of Ethics.
   - The authors should make sure to preserve anonymity (e.g., if there is a special consideration due to laws or regulations in their jurisdiction).

10. **Broader Impacts**

    Question: Does the paper discuss both potential positive societal impacts and negative societal impacts of the work performed?

    Answer: [Yes]

    Justification: We are discussing potential broader impacts of our work in a dedicated section.

    Guidelines:

    - The answer NA means that there is no societal impact of the work performed.

- If the authors answer NA or No, they should explain why their work has no societal impact or why the paper does not address societal impact.
- Examples of negative societal impacts include potential malicious or unintended uses (e.g., disinformation, generating fake profiles, surveillance), fairness considerations (e.g., deployment of technologies that could make decisions that unfairly impact specific groups), privacy considerations, and security considerations.
- The conference expects that many papers will be foundational research and not tied to particular applications, let alone deployments. However, if there is a direct path to any negative applications, the authors should point it out. For example, it is legitimate to point out that an improvement in the quality of generative models could be used to generate deepfakes for disinformation. On the other hand, it is not needed to point out that a generic algorithm for optimizing neural networks could enable people to train models that generate Deepfakes faster.
- The authors should consider possible harms that could arise when the technology is being used as intended and functioning correctly, harms that could arise when the technology is being used as intended but gives incorrect results, and harms following from (intentional or unintentional) misuse of the technology.
- If there are negative societal impacts, the authors could also discuss possible mitigation strategies (e.g., gated release of models, providing defenses in addition to attacks, mechanisms for monitoring misuse, mechanisms to monitor how a system learns from feedback over time, improving the efficiency and accessibility of ML).

11. **Safeguards**

    Question: Does the paper describe safeguards that have been put in place for responsible release of data or models that have a high risk for misuse (e.g., pretrained language models, image generators, or scraped datasets)?

    Answer: [NA]

    Justification: This paper does not pose such risks.

    Guidelines:

    - The answer NA means that the paper poses no such risks.
    - Released models that have a high risk for misuse or dual-use should be released with necessary safeguards to allow for controlled use of the model, for example by requiring that users adhere to usage guidelines or restrictions to access the model or implementing safety filters.
    - Datasets that have been scraped from the Internet could pose safety risks. The authors should describe how they avoided releasing unsafe images.
    - We recognize that providing effective safeguards is challenging, and many papers do not require this, but we encourage authors to take this into account and make a best faith effort.

12. **Licenses for existing assets**

    Question: Are the creators or original owners of assets (e.g., code, data, models), used in the paper, properly credited and are the license and terms of use explicitly mentioned and properly respected?

    Answer: [Yes]

    Justification: We used the Kubric generator with the built-in asset library and a range of pretrained models. We cited the sources of all data and implementations that we used.

    Guidelines:

    - The answer NA means that the paper does not use existing assets.
    - The authors should cite the original paper that produced the code package or dataset.
    - The authors should state which version of the asset is used and, if possible, include a URL.
    - The name of the license (e.g., CC-BY 4.0) should be included for each asset.
    - For scraped data from a particular source (e.g., website), the copyright and terms of service of that source should be provided.

- If assets are released, the license, copyright information, and terms of use in the package should be provided. For popular datasets, `paperswithcode.com/datasets` has curated licenses for some datasets. Their licensing guide can help determine the license of a dataset.
- For existing datasets that are re-packaged, both the original license and the license of the derived asset (if it has changed) should be provided.
- If this information is not available online, the authors are encouraged to reach out to the asset's creators.

13. **New Assets**

    Question: Are new assets introduced in the paper well documented and is the documentation provided alongside the assets?

    Answer: [Yes]

    Justification: The synthetic data we generated for the paper is described in the paper, and published with the code used to generate it.

    Guidelines:

    - The answer NA means that the paper does not release new assets.
    - Researchers should communicate the details of the dataset/code/model as part of their submissions via structured templates. This includes details about training, license, limitations, etc.
    - The paper should discuss whether and how consent was obtained from people whose asset is used.
    - At submission time, remember to anonymize your assets (if applicable). You can either create an anonymized URL or include an anonymized zip file.

14. **Crowdsourcing and Research with Human Subjects**

    Question: For crowdsourcing experiments and research with human subjects, does the paper include the full text of instructions given to participants and screenshots, if applicable, as well as details about compensation (if any)?

    Answer: [Yes]

    Justification: Screenshots of the experiment are included in the supplemental material.

    Guidelines:

    - The answer NA means that the paper does not involve crowdsourcing nor research with human subjects.
    - Including this information in the supplemental material is fine, but if the main contribution of the paper involves human subjects, then as much detail as possible should be included in the main paper.
    - According to the NeurIPS Code of Ethics, workers involved in data collection, curation, or other labor should be paid at least the minimum wage in the country of the data collector.

15. **Institutional Review Board (IRB) Approvals or Equivalent for Research with Human Subjects**

    Question: Does the paper describe potential risks incurred by study participants, whether such risks were disclosed to the subjects, and whether Institutional Review Board (IRB) approvals (or an equivalent approval/review based on the requirements of your country or institution) were obtained?

    Answer: [Yes]

    Justification: The study in this paper does not pose any particular risk on participants. IRB approval exists.

    Guidelines:

    - The answer NA means that the paper does not involve crowdsourcing nor research with human subjects.

- Depending on the country in which research is conducted, IRB approval (or equivalent) may be required for any human subjects research. If you obtained IRB approval, you should clearly state this in the paper.
- We recognize that the procedures for this may vary significantly between institutions and locations, and we expect authors to adhere to the NeurIPS Code of Ethics and the guidelines for their institution.
- For initial submissions, do not include any information that would break anonymity (if applicable), such as the institution conducting the review.